Santos-Martin, David; Lemon, Scott. (2016). Simplified Modeling of Low Voltage Distribution Networks for PV Voltage Impact Studies. *IEEE Transactions on Smart Grid*, 7(4), pp.: 1924-1931.

DOI: https://doi.org/10.1109/TSG.2015.2500620

Simplified Modeling of Low Voltage Distribution Networks for PV Voltage Impact Studies

David Santos-Martin and Scott Lemon, *Student Member, IEEE*

***Abstract*—Distributed generation is increasingly being integrated into distribution networks worldwide, presenting new challenges for network operators and planners. In particular, the introduction of photovoltaic (PV) generation at the low voltage (LV) level has highlighted the ongoing need for more extensive and detailed modeling to quantify the full extent and nature of potential impacts. While a number of approaches have been developed to address the size of this problem, the most accurate and comprehensive approach is to carry out simulations for the entire network across multiple scenarios. However, this task is computationally complex and requires significant amounts of data. To address this challenge, this paper presents a simplified and computationally efficient methodology based around a two-bus equivalent model, which may be used to estimate the maximum voltage in an LV area due to PV generation over time. The developed model is validated against a full three-phase power flow approach for a real-world distribution network comprising 10 213 LV network areas. Furthermore, to highlight its utility, the model is used in a case study examining the effectiveness of reactive power injection for mitigating overvoltage due to PV generation.**

***Index Terms*—Distribution network, photovoltaic systems, power system modeling, reactive power, voltage impact.**

I. Introduction

DISTRIBUTED generation (DG) and, in particular, photovoltaic generation (PV) is increasingly being integrated into distribution networks (DN). Currently, over 180 GW of PV generation has been installed worldwide, with an average of over 120 W per inhabitant in Europe in 2014. This generation comprises small residential schemes, which make up 25% of total installed capacity in Europe, and larger commercial plants at the low- and medium-voltage levels. As the price of PV components continues to decrease, this trend of accelerating PV penetration levels is expected to continue, with grid parity being reached in a number of countries [1].

However, the introduction of such distributed generation sources leads to new challenges and concerns for distribution system operators (DSO) and planners worldwide. Traditionally, at the low- and medium-voltage levels such as 400V and 11kV, distribution networks have predominantly been comprised of passive loads. The flow of real power has thus been largely unidirectional, flowing down from distribution transformers to the connected loads, thereby allowing control and protection schemes to be defined unambiguously. As DG is introduced and power is injected back into the network, the resulting reverse power flows may initially lead to overvoltage issues and also, at high penetration levels, overloading issues. These issues may in turn necessitate more complex control and protection schemes at both the network level and within individual DG units.

DSOs are consequently faced with two key challenges under this changing paradigm: to understand the impact of DG across their networks; and to ascertain the best methods for managing/mitigating these impacts to ensure compliance with standards and regulations [2], [3]. In many cases this is particularly difficult given the accelerating rate of PV uptake and the immediate need to introduce planning criteria. To address these challenges, detailed studies and simulations must be carried out for each section of the network, across multiple current and future scenarios, and with sufficient spatiotemporal resolution. A number of such large scale PV integration studies have been carried out worldwide as in [4] and [5].

In general, the impact studies required are technically and computationally complex, necessitating the development and creation of new and more detailed models of LV network elements, household load, PV generation, and their interconnection. In many cases the models and data required are not available, not complete, or not in a form readily usable for such studies at this voltage level [6].

A number of approaches have been adopted to perform these studies, including analyses of only the worst-case scenarios [7], or broader probabilistic analyses of all likely network configurations and generation scenarios [8]–[10]. To simplify the process of analyzing the impact of PV generation across a DN, a common approach is to only model a subset of the areas, which are considered 'representative' of different sections of the network. However, this methodology precludes a detailed understanding of the impact within every LV area, and introduces a degree of uncertainty that is not easy to assess.

Undoubtedly, the most accurate and comprehensive approach is to simulate the entire network using quasi-steady state power flows or dynamic simulations, performed over extended time periods at a high temporal resolution, and across a diverse range of scenarios. However, the computational

burden and data requirements for such an approach are immense. For example, a European-style distribution network with 500,000 customers may have on the order of 10,000 MV/LV distribution transformers and 15,000 feeders. Simulating a single year with only 10 minute resolution, and recording the voltage and current at each bus in the network, may require several weeks of computing time for a single workstation, and will produce terabytes of data.

It is proposed that a simplified model can be used to accurately estimate the magnitude of overvoltage within LV areas with only limited data and in a small amount of time. Such data is limited to the length and impedance of each branch and the parent branch to which they are connected, as well as the load/generator ratings and parent connection. It can thus be implemented as a simple analytical spreadsheet script operating directly on raw tabular data, without having to first convert data to a specific format and then interface with a full power flow solver. This in turn allows DSOs to quickly identify and prioritize those areas which require more detailed analysis and studies. Furthermore, such a model can be used to simplify the computational complexity of carrying out integrated studies incorporating the entirety of the MV and LV networks.

The idea of creating simplified or aggregated network models for analyzing the impact of DG is not new. In [11], a lumped load model is developed for estimating voltage drop and power in balanced three phase systems with uniformly distributed loads. In [12], a method is proposed for aggregating a wind power plant (WPP) collector system. This method is utilized in [13] for computing the equivalent collector system impedance of distribution- and transmission-connected PV plants. The resulting 'single-machine equivalent representation' is used in bulk-system load flow simulations for estimating real and reactive power losses in lines [14]. In [14] and [15] a methodology to reduce distribution feeders for simplified loss analysis at the distribution level is presented and validated for snapshot and time series simulations. The existence of these recent studies highlights the need for the development of simplified models, and in particular those for analyzing voltage impacts due to DG.

Among the most relevant studies for the planning or control of PV generation in distribution networks are those related to the estimation of steady state voltage. Many of the simplified models currently proposed focus on finding the equivalent impedance of a collector system, which effectively averages load/generation and consequently voltage across an area [12], [14], [15]. As such, they cannot be used for the computation of voltage extremes within each area and are thus unsuitable for voltage impact studies at the LV level. In [14] an approach is developed for the partial reduction of branches in a network, predicated on the assumption of fixed current, balanced loads and balanced line impedances. While this approach has the key advantage of allowing voltage extrema and line losses to be computed at the buses of interest, it still requires the use of an iterative power flow solver.

The derivation, validation and application of a simplified model forms the focus of this paper. Initially the two-bus model is presented, including the formulation of an analytic expression for voltage rise across the network. An approach is then described for reducing an LV distribution network of arbitrary complexity to this two-bus form. The resulting model is validated against a full quasi-steady state power flow using the current-injection method, before being applied to an analysis of the utility of reactive power for managing overvoltage issues.

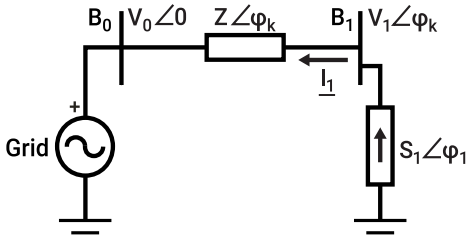

Fig. 1. Two-bus equivalent model for an LV area.

II. Model Formulation

A. Two-Bus Equivalent Model

The two-bus model (TBM) is comprised of three components: a slack bus with a defined reference voltage, an equivalent network impedance, and an aggregated load and PV generation model. As shown in Fig. 1, bus B_0 is the slack bus, representing the connection of the grid at a fixed reference voltage $\underline{V_0}$ with infinite short-circuit power. Bus B_1 connects the net generation or consumption to the grid through an equivalent impedance.

The voltage $\underline{V_1}$ at the load and generation bus B_1 can be expressed as a function of the reference voltage $\underline{V_0}$, the equivalent network impedance $\underline{Z}$ and the net complex injected power $\underline{S_1}$.

$$\underline{V_1} = \underline{V_0} + \underline{Z} \cdot \underline{I_1} = \underline{V_0} + \underline{Z} \cdot \frac{\underline{S_1}^*}{\underline{V_1}^*} \tag{1}$$

The voltage at the load and generation bus can be expressed as $\underline{V} = \underline{V_1}/\underline{V_0}$, being defined relative to the reference bus. Substituting for $\underline{V_1}$ in (1) yields,

$$\underline{V} = 1 + \underline{Z} \cdot \frac{\underline{S_1}^*}{V_0^2} \cdot \frac{1}{\underline{V}^*} \tag{2}$$

Where the voltage $\underline{V}$ can be considered as the per-unit value of $\underline{V_1}$, while the other variables in the equation can be expressed in either per-unit or physical values, as the base changes will cancel out.

A simplified expression for $\underline{V}$ can subsequently be obtained by defining a new variable $\underline{\alpha}$ in terms of two key properties of the network: the short-circuit ratio (SCR $= S_k/S_1$) and the angle delta ($\delta = \varphi_k - \varphi_1$). In these expressions S_k is the short-circuit power at bus B_1, S_1 is the complex power injected at B_1, φ_k is the total impedance angle and φ_1 is the complex power angle.

$$\underline{\alpha} = \underline{Z} \cdot \frac{\underline{S_1}^*}{V_0^2} = \frac{S_1}{V_0^2/Z}\underline{/\varphi_k - \varphi_1} = \frac{S_1}{S_k}\underline{/\delta} = \frac{1}{\text{SCR}}\underline{/\delta} \tag{3}$$

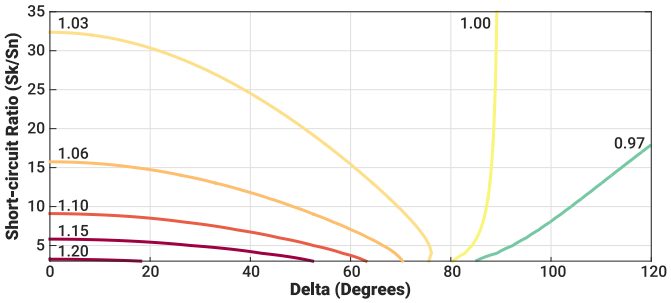

Fig. 2. Voltage profile for the two-bus model as a function of the short-circuit ratio (SCR $= S_k/S_1$) and the angle delta ($\delta = \varphi_k - \varphi_1$).

Substituting this new variable into (2) and multiplying throughout by $\underline{V}^*$ yields the simple equation,

$$V^2 = \underline{V}^* + \underline{\alpha} \tag{4}$$

This can be solved for $\underline{V}$ by splitting the real and imaginary parts and applying the quadratic formula to each. The resulting analytic solution for $\underline{V}$ is given by (5), and is expressed solely in terms of the real α_R and imaginary α_I parts of $\underline{\alpha}$.

$$\underline{V} = 1/2 + \sqrt{1/4 - \left(\alpha_I^2 - \alpha_R\right)} + j\alpha_I \tag{5}$$

From (3) it can be seen that α_R and α_I are readily expressible in terms of the complex power $\underline{S_1} = P + jQ$ and the network impedance $\underline{Z} = R + jX$.

$$\begin{aligned} \alpha_R = \mathrm{Re}\{\underline{\alpha}\} &= \frac{P \cdot R + Q \cdot X}{V_0^2} \\ \alpha_I = \mathrm{Im}\{\underline{\alpha}\} &= \frac{P \cdot X - Q \cdot R}{V_0^2} \end{aligned} \tag{6}$$

The analytic solution of (5) can be visualized as a set of contours, as shown in Fig. 2. These depict the voltage profile of $\underline{V}$ as a function of the short-circuit ratio (SCR $= S_k/S_1$) and the angle delta ($\delta = \varphi_k - \varphi_1$). These plots show the influence of different variables, including the level of PV generation S_1, the generation power factor φ_1 and the network characteristics S_k and φ_k on the overall voltage impact in a way that is easy to understand. In addition, they intimate the potential of different mitigation strategies such as active power curtailment (reducing S_1) or reactive power injection for reducing overvoltage. Note that the angle delta increases when the reactive power injection increases as $\delta = \varphi_k - (-\varphi_1) = \varphi_k + \varphi_1$. While S_1 is effectively the injected power, it could also be understood as the penetration level.

B. LV Area Simplification

A typical European-style distribution network LV area, common to many countries, is comprised of a single three-phase transformer supplying one or more feeders and a set of attached loads, as shown in Fig. 3. Each feeder is made up of multiple three-phase, four-wire line/cable sections and may serve multiple customer types including residential, commercial and/or industrial loads. Each load, and attached PV generator, may be connected across the different phases and neutral as a single or multiple phase system. The number of

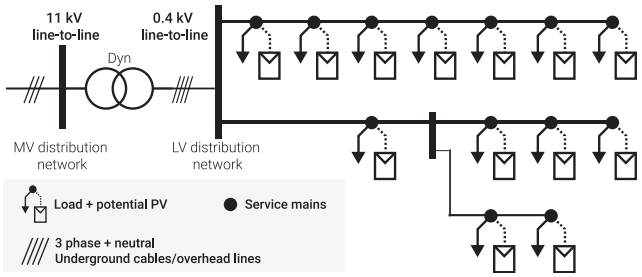

Fig. 3. Example of a typical distribution network LV area.

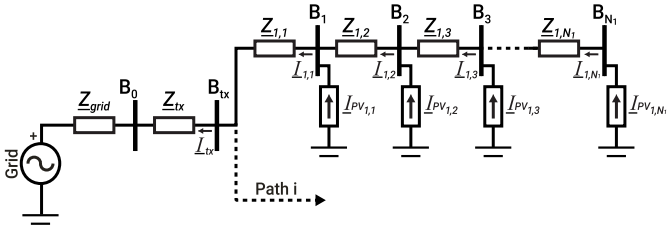

Fig. 4. Single line diagram of a path through an LV network area.

customer units and the complexity of the network topology for these LV network areas may vary widely across a distribution network, ranging from a single to several hundreds of units, with a wide variety in the number of main feeders and lateral branches.

Consider a single path through a radial LV area, running from the distribution transformer to a single end bus, as shown in Fig. 4. A single feeder may contain multiple paths if there are a number of lateral branches. The voltage level at each bus along this path depends on the impedance from it to the slack bus B_0, and the total current flowing through those impedances. Assuming a balanced scenario with equal PV generation connected across all three phases at each bus, the maximum voltage will occur at the end of each path. To reduce the network to its equivalent two-bus representation, an equivalent impedance can be found for each path that approximates the maximum voltage at the end of that path under these assumptions. The equivalent impedance that produces the highest overvoltage for a given generation scenario is then used to model the network.

The voltage difference between the end of the i^{th} path and the reference slack bus, B_0, can be expressed as the sum of the individual voltage differences across each of the N_i impedances in that path, as in (7).

$$\underline{\Delta V_i} = \underline{Z_{tx}}\underline{I_{tx}} + \sum_{j=1}^{N_i} \underline{Z_{i,j}}\underline{I_{i,j}} \tag{7}$$

Where, $\underline{Z_{tx}}$ is the per-phase series transformer impedance referred to the LV side, $\underline{I_{tx}}$ is the total current flowing through the transformer, and $\underline{Z_{i,j}}$ is the positive sequence impedance of the cables or overhead lines connected to j^{th} bus in the i^{th} path. Note that if the grid is being modeled as a Thévenin equivalent voltage source, then (7) must also include the voltage drop across the equivalent series impedance of the grid, $\underline{Z_{grid}}$, referred to the LV side of the transformer. In addition,

the current $\underline{I}_{i,j}$ flowing through the impedance $\underline{Z}_{i,j}$ is given by the sum of all net currents injected downstream $\underline{I}_{PV_{i,k}}$, computed as the difference of PV generation and load consumption, as in (8).

$$\underline{I}_{i,j} = \sum_{k=j}^{N_i} \underline{I}_{PV_{i,k}} \tag{8}$$

For example, the current flowing through the impedance $\underline{Z}_{i,1}$ is given by $\underline{I}_{i,1} = \underline{I}_{PV_{i,1}} + \underline{I}_{PV_{i,2}} + \cdots + \underline{I}_{PV_{i,N_i}}$, while for the impedance $\underline{Z}_{i,N_i}$ it is $\underline{I}_{i,N_i} = \underline{I}_{PV_{i,N_i}}$.

Given the unequal injected current at each bus, a solution to this equation is largely intractable using analytical methods, and thus a numerical power flow approach is commonly adopted. However, for the purposes of developing an analytic model for approximating the absolute maximum overvoltage within a network area, a number of assumptions can be made. Due to the limited geographic size of an LV area it can be assumed that each PV generator is subject to the same irradiance, at low temporal resolution. For the purposes of network screening it can be assumed that, for a given penetration level, the PV generators are uniformly distributed over the network and across all three phases, with each generator having the same rated output. Furthermore, as the key value of interest is the maximum theoretical steady state voltage at times of peak generation, the load variability across sites can be assumed to be similar and the voltage dependence disregarded. With these assumptions the results are only valid under balanced conditions, with a corresponding level of accuracy. However, this is considered sufficient for the purposes of pre-screening and ranking networks for further analysis and more detailed unbalanced studies.

Under these assumptions, the net injected current at each bus can be assumed equal, and is given by the single time-variant variable $\underline{I}$. The voltage drop across a given branch can subsequently be expressed in (9) in terms of the current $\underline{I}$ and the number of power sources $n_{i,j}$ injecting current downstream of the j^{th} bus in the i^{th} path, similar to the concept described in [16]. Note that this includes any power sources connected on lateral branches off the main path.

$$\underline{\Delta V}_i \approx \underline{Z}_{tx}\underline{I}_{tx} + \sum_{j=1}^{N_i} \underline{Z}_{i,j}\left(n_{i,j}\underline{I}\right) \tag{9}$$

In accordance with Kirchhoff's current law, and under the above assumptions, the current flowing through the transformer $\underline{I}_{tx}$ is equal to the sum of all N_{total} injected currents $\underline{I}$. Substituting the value for $\underline{I}$ into (9), a new expression can be derived for $\underline{\Delta V}_i$ in terms of the total transformer current $\underline{I}_{tx}$ and an equivalent impedance $\underline{Z}_{eq}$.

$$\underline{\Delta V}_i \approx \left(\underline{Z}_{tx} + \frac{1}{N_{total}} \sum_{j=1}^{N_i} \underline{Z}_{i,j} n_{i,j}\right) \underline{I}_{tx} \tag{10}$$

From (10), an equivalent impedance Z_{eq} (11) can be found for each path in the network that approximates the maximum voltage at the end of that path. This is analogous to the equivalent sum-impedance presented in [17], although here (10) accounts for all paths throughout the network and not only a single feeder without laterals.

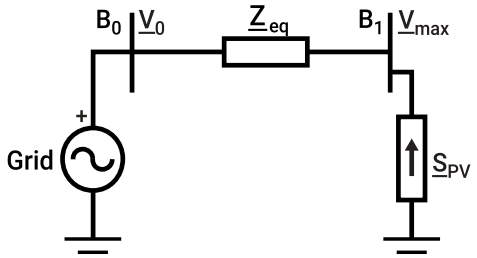

Fig. 5. Two-bus equivalent model of a full network after reduction.

$$\underline{Z}_{eq_i} = \underline{Z}_{tx} + \frac{1}{N_{total}} \sum_{j=1}^{N_i} \underline{Z}_{i,j} n_{i,j} \tag{11}$$

The overall equivalent impedance $\underline{Z}_{eq}$ used to represent the network is the one that, within the set of all path impedances $\boldsymbol{Z_P}$, gives the maximum area voltage ($\underline{V}_{area,max}$) calculated using (5),

$$\underline{Z}_{eq} = \underset{\underline{Z}_{eq_i} \in \boldsymbol{Z_P}}{\operatorname{argmax}} \underline{V}_{area,max} \tag{12}$$

It is important to note that by this definition the equivalent impedance $\underline{Z}_{eq_i}$, and in turn the path in which the maximum voltage occurs, may vary across different power factor scenarios in some cases. Although $\underline{Z}_{eq}$ can be approximated by using the $\underline{Z}_{eq_i}$ value with the maximum magnitude, this may lead to a slight increase in the error as discussed in the model validation section. This is due to the fact that the voltage increase also depends on the angle of the impedance.

To match the analytic form described earlier in the formulation of the two-bus model, the total net injected power S_{PV} can be expressed as the sum of the power injected at each bus S_i, such that $S_{PV} = \sum \underline{S}_i$.

As evident in Fig. 5, the reduced LV area model is equivalent to the two-bus model described earlier, and is thus amenable to analysis with the same equations (5-6) across different scenarios of net injected power.

III. Model Validation

The simplified equivalent model was validated using data from a real distribution network comprised of 10,213 LV network areas. Each area has a single 11/0.415 kV delta-wye transformer, one or more feeders, and one or more attached loads. The areas are connected to a grid with a short-circuit power of 96.2 MVA and an X/R ratio of 7. Table I presents an overview of the DN using a set of statistical metrics to summarize a range of network characteristics. For these metrics the total impedance and short-circuit power have been calculated considering: the Thévenin equivalent impedance of the grid, and the impedances of the transformer, lines/cables and service mains. The diversity and number of LV networks considered allows for a good estimate to be obtained regarding the error and performance that can be expected using the model in similar networks.

TABLE I
DISTRIBUTION NETWORK STATISTICS

	Units	Percentiles								
		p1	**p5**	**p10**	**p25**	**p50**	**p75**	**p95**	**p99**	**p100**
Transformer rating (S_{tx})	kVA	7.5	10	15	30	50	300	500	1000	1500
Number of loads	-	1	1	1	1	3	24	84	127	347
Equivalent impedance magnitude (Z_{eq})	Ω	0.0175	0.0346	0.0474	0.0683	0.177	0.301	1.45	1.96	2.98
Equivalent impedance angle (φ_k)	Degrees	21.5	27.6	28.7	36.1	40.7	51.3	56.2	63.5	74.1
R/X ratio	-	0.498	0.67	0.754	0.801	1.16	1.37	1.91	2.54	6.26
Z_{eq}/Z_{tx}	p.u.	1.01	1.03	1.03	1.08	1.21	2.17	3.92	5.56	19.4
Short-circuit power (S_k[1])	MVA	0.0878	0.119	0.242	0.572	0.973	2.52	4.98	9.86	16.8
S_k/S_{tx}	p.u.	4.00	5.88	7.27	10.7	16.0	19.3	20.6	20.7	21.7

[1] Seen from the generation/load bus, thus including transformer, line/cable and service mains impedances

A. Validation Methodology

For each of the 10,213 LV areas described above, a full quasi-steady state three-phase power flow simulation was carried out for one summer month with a temporal resolution of 10 minutes. The simulation process was repeated for 12 different scenarios, encompassing 4 different penetration levels (10, 30, 50 and 100%) defined as the total installed PV capacity in the area as a percentage of the transformer rating, and 3 different generation power factors (1, 0.95 and 0.9 underexcited). The total installed capacity was divided equally between all PV generation sites, as shown in Fig. 3.

The PV generation at each site was subsequently computed using the rated PV generator capacity and real irradiance data from a local pyranometer within the network. A simplified linear version of the PVUSA AC rating method, as described in [18], was used to convert irradiance values into per-unit power values, in which only the dependency of output power on irradiance was considered. The irradiance data was normalized and a typical conversion factor of 97% for PV systems was applied.

To quantify the error introduced by the assumption in the model formulation that the loads have similar variability with respect to both time and voltage, two contrasting cases were simulated. In the first case, the load at each site was set to zero, with no temporal or voltage dependence, so as to estimate the theoretical absolute maximum voltage. In the second case, the impacts of both the temporal and voltage characteristics of residential loads were analyzed.

In the more detailed case the validation was carried out on a subset of 3089 of the networks containing only residential loads. The load profile for each site was selected randomly from a database of 2214 load profiles over 1 year from smart meters within the same network. The load itself was modeled such that the consumed current is dependent on the applied voltage in accordance with the commonly used static polynomial ZIP model [19]. The coefficients selected for the ZIP model were assumed constant, with active power coefficients ($Z_p = 0.51$, $I_p = 0.04$, $P_p = 0.45$) and reactive power coefficients ($Z_q = 0.96$, $I_q = -0.57$, $P_q = 0.60$) based on average residential values from [20], and a displacement power factor of 0.97. The ZIP coefficients describe the nature of different appliance types within the load profile - for example, water heating loads are constant impedance.

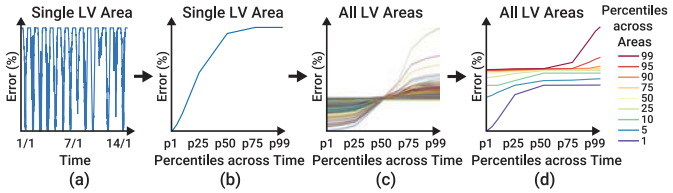

Fig. 6. Methodology for computing the simplified model error across time and for all LV networks. (a) Model error for a single LV area. (b) Percentile error across time for a single LV area. (c) Percentile error across time for all LV areas. (d) Percentile error across time and LV areas.

The maximum voltage magnitude, hereafter referred to as the voltage, at each instance in time was then compared with that estimated using the two-bus model. To obtain a useful comparison across time and for all of the LV networks, percentiles were computed along both dimensions as outlined in Fig. 6. First, the model error was computed every 10 minutes for each LV network by calculating the difference between the maximum voltage calculated using the full and simplified models respectively. The temporal dimension was then reduced by computing the percentile error across time. Finally, the percentile errors for all LV networks were collected and a second percentile computed across all of the areas.

B. Validation Results

The resulting error between the full power flow simulation and the simplified two-bus model with no load and with load are shown in Fig. 7 and Fig. 8 respectively for the 30% and 100% penetration level scenarios. The vertical axis of each subplot shows the percentage error in maximum voltage calculated, while the horizontal axis shows the percentiles across time. Each of the curves corresponds to a percentile computed across all LV network areas.

In Fig. 7 it can be seen that for the no load case, as the penetration level is increased or the power factor is decreased, the error between the full and simplified models increases. In general, for low penetration levels the simplified model will slightly overestimate the maximum voltage, thus providing a conservative measure of the impacts. Across all scenarios the absolute error in the estimated maximum voltage never exceeds 0.5% at any point in time for 99% of the areas. Significantly smaller error bounds can be obtained by considering only a subset of time values or less complex network areas.

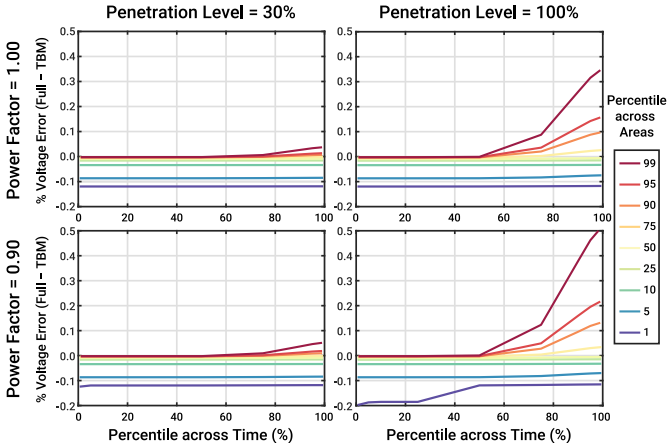

Fig. 7. Error between the full power flow simulation and the simplified two-bus model across time for all LV networks with only PV generation and no load, as a function of penetration levels and underexcited power factors.

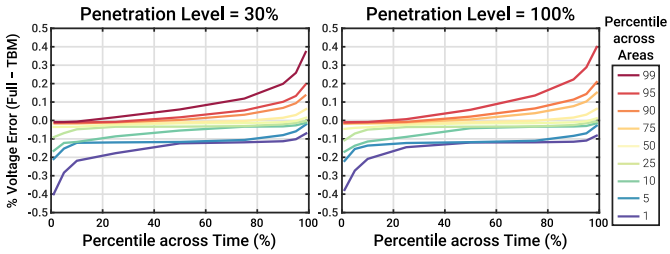

Fig. 8. Error between the full power flow simulation and the TBM across time for residential LV networks with PV generation and load, for 0.9 power factor.

Furthermore in Fig. 8 for the case with load in residential networks, at high penetration levels similar error performance can be observed due to the generation dominating. However, at lower penetration levels a higher error level occurs, but remains within the same 0.5% error bounds. Subsequently, it can be concluded that the simplified model performs well with realistic generation and load time series across multiple power factor and penetration level scenarios.

The maximum permissible voltage deviation for LV networks may be defined in terms of an absolute voltage magnitude limit, for example 230 V nominal +/-10% as in IEC 60038 [21]. Alternatively, it may be defined relative to the operating voltage of the LV network without power flowing, for example a maximum voltage change of 3% as in VDE-AR-N 4105 [22]. The advantage of the latter approach is that it is independent of the operating point of the transformer taps, which may vary across networks.

For the distribution network considered, the nominal voltage is 230 V. The transformers are operated with a fixed tap at 415 V phase-to-phase, or 239.6 V phase-to-neutral (230 V + 4%). This is done by DSOs in some countries to account for the voltage drop along feeders due to loads.

To quantify the overvoltage due to PV generation the maximum voltage criteria was used. Two limits were considered: 3% and 6% relative to the operating voltage (239.6 V), corresponding to 246.8 V (230 V + 7%) and 254 V (230 V + 10.4%) respectively. To simplify interpretation of

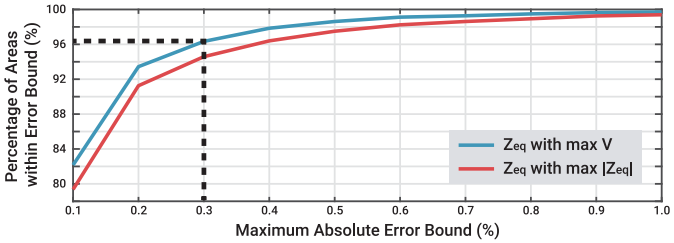

Fig. 9. Percentage of areas within defined error bounds for a scenario of 100% penetration and 0.9 power factor using Z_{eq} that gives the maximum voltage and that with the maximum magnitude.

Load Count \ Transformer Rating (kVA)	0-10	11-50	51-100	101-200	201-500	501-1000	>1000
>200	-	-	-	-	0 (0/1)	70 (7/10)	-
101-200	-	-	-	0 (0/2)	22 (47/212)	53 (17/32)	-
51-100	-	-	0 (0/1)	0 (0/343)	14 (134/985)	56 (15/27)	-
21-50	-	0 (0/12)	2 (1/45)	2 (12/548)	11 (43/391)	40 (22/55)	-
11-20	-	0 (0/50)	0 (0/74)	5 (6/125)	12 (18/156)	39 (17/44)	-
6-10	-	0 (0/251)	0 (0/85)	1 (1/73)	6 (6/104)	35 (7/20)	-
1-5	0 (0/520)	0 (0/4323)	0 (0/607)	1 (3/461)	2 (10/431)	4 (8/215)	0 (0/10)

Fig. 10. Percentage of areas (with absolute number in parenthesis) that have an error above 0.3%, grouped by transformer rating and number of loads.

the results, the overvoltage values are defined on a per unit basis relative to the operating voltage, such that 1 p.u. corresponds to 239.6 V, 1.03 p.u. corresponds to 246.8 V and 1.06 p.u corresponds to 254 V.

The acceptable error in the model was deemed to be 10% of the maximum 3% deviation, corresponding to a maximum absolute error bound of 0.3%. In Fig. 9 it can be seen that for the scenario with the highest error levels (100% penetration and 0.9 power factor), 96.3% of the areas fall within this error bound for all time values.

C. Criteria for Using the Simplified Model

For the DN under study, the correlation between the model error and network characteristics was investigated. All of the areas with a maximum absolute error exceeding the bound of 0.3% at any time for the 100% penetration level and 0.9 power factor were grouped based on the corresponding transformer rating and number of loads/generators. As evident in Fig. 10, as the size and complexity of the network increases, with an increase in the transformer rating and load count, so too does the degree of error in the model. Thus, while the simplified model has very good performance for small to medium areas, for larger areas it may prove more convenient and reliable to use a detailed network model.

Unfortunately, it is not possible to define a perfect rule for when the simplified model may be used with an acceptable error level using readily observable network characteristics such as load count. If it proves necessary to exactly define the error bounds of the simplified model for analyzing a specific DN, then the results of the model can be compared with those of a full power flow solver for a single conservative case.

Subsequently, the model may safely be applied to the DN for multiple time series and scenarios.

D. Computation Time

The simplified approach was observed to be over two-orders of magnitude faster than the current injection method during the validation process. All simulations were run on a single 2.7 GHz core of a workstation utilizing 16 GB of RAM. The full approach required approximately 12.3 hours to run all scenarios while the simplified approach required only 1.5 minutes, without the need for power flow software. While these timings depend heavily on the computer hardware used and the software implementation of the algorithms, they indicate the order of the speedup that would be observed in practice. This increase in speed is particularly valuable when simulating integrated MV to LV level models, and running a large number of scenarios for planning purposes.

IV. Case Study

The analysis of mitigation measures to limit the voltage rise has been presented in multiple studies as in [23] and [24]. To demonstrate the utility of the simplified model, a case study was developed for the described DN in which the effectiveness of using reactive power to mitigate overvoltage was analyzed. For each area, the calculated equivalent impedance was used to find the corresponding short-circuit ratio (SCR) and delta (δ) properties given the 12 scenarios of PV penetration and power factor. The models and assumptions regarding generation and load are consistent with those used during validation.

These results were plotted against the voltage profile for the two-bus model, showing the maximum per unit voltage estimated for each area and for each scenario as in Fig. 2. Each of the 10,213 points corresponds to one of the modeled areas, while the heat map shading corresponds to the density of points in that region.

In Fig. 11 it can be seen that overvoltage values $\underline{V}$ above 1.03 p.u. and 1.06 p.u. are very rare for low penetration levels such as 10%, while for penetration levels of 100% most of the areas show overvoltage. When PV sources absorb reactive power, the voltage level always becomes smaller. As the underexcited power factor is changed to 0.95 and 0.9, each area, as indicated by a dot, is shifted horizontally by a factor equal to the *arccosine* of the power factor, or 18.2 and 28.8 degrees respectively. However, the effect of this shift and the corresponding reactive power absorption ultimately depends on the starting position of the area. For those areas with an overvoltage above 1.03 p.u. or 1.06 p.u., and with a low starting delta value (low φ_k), the dots will move nearly parallel to the voltage contours, thus resulting in a small voltage reduction. Alternatively, for areas with high starting delta values (high φ_k) a small amount of reactive power will allow for a significant voltage reduction.

Despite the common belief that providing PV inverters with feasible reactive power capability will eliminate overvoltage issues, its effectiveness at mitigating overvoltage in LV areas cannot be assumed. As shown in Fig. 11 and in Table II, given a conservative overvoltage bound of 1.03 p.u., for moderate

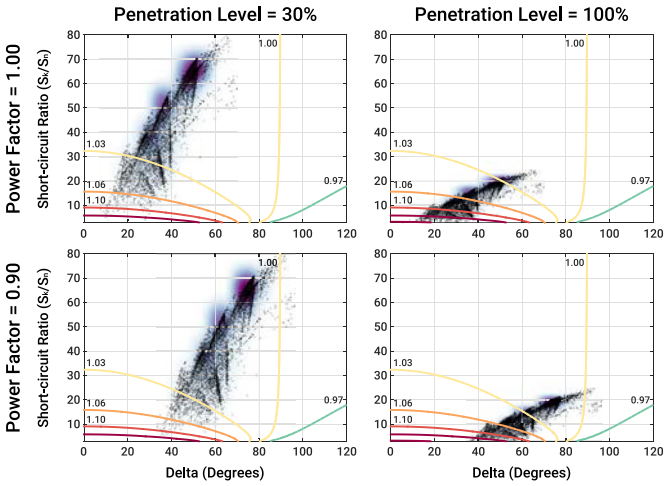

Fig. 11. Comparison of overvoltage impact for different penetration levels (30 and 100%) and power factors (1 and 0.90 inductive). Each dot represents one of the 10,213 LV areas, with the background shading corresponding to the density of points in that region.

TABLE II
Overvoltage Percentiles as a Function of the Generation Penetration Level and Power Factor

Penetration Level	Percentiles	Power Factor 1	0.95	0.9
30	p5	1.009	1.005	1.003
	p50	1.014	1.010	1.008
	p75	1.023	1.017	1.014
	p95	1.043	1.034	1.029
	p99	1.064	1.052	1.045
	p100	1.197	1.174	1.158
50	p5	1.014	1.008	1.005
	p50	1.023	1.016	1.013
	p75	1.037	1.028	1.023
	p95	1.069	1.054	1.047
	p99	1.103	1.083	1.072
	p100	1.302	1.265	1.239
100	p5	1.028	1.015	1.008
	p50	1.046	1.032	1.025
	p75	1.071	1.053	1.045
	p95	1.130	1.102	1.087
	p99	1.190	1.151	1.132
	p100	1.516	1.446	1.397

* Values higher than 1.03 p.u. or 1.06 p.u. are shown shaded.

penetration levels up to 30% there is no need to provide reactive power capability. At these levels, approximately 90% and 99% of the areas have no overvoltage above 1.03 p.u. and 1.06 p.u. respectively.

Alternatively, for extremely high penetration levels the effect of operating the inverter with an underexcited power factor of 0.9 does not seem to fully mitigate the problem for either the 1.03 p.u. or 1.06 p.u. overvoltage limits. More than 50% of the areas would still have overvoltage above 1.03 p.u., and more than 25% overvoltage above 1.06 p.u. with this power factor. Only an extra 25% would enter the zone with an overvoltage less than 1.03 p.u., and 15% an overvoltage less than 1.06 p.u.. Furthermore, for intermediate penetration levels, only a small percentage of areas would be below the bound levels due to the reactive power absorption.

V. Conclusion

An approach has been proposed for reducing an LV network area to a two-bus model, which can be used for estimating the overvoltage impact due to PV across a distribution network. This model can be used by DSOs' planners for screening and ranking those networks in which overvoltage is expected to occur, and thus require further, more detailed analysis. In turn, this allows networks to be prioritized for which more detailed data should be collected, and full power flow models created and run. Such power flow simulations should, in most cases, consider the impact of network unbalance and the allocation of generation/loads.

Furthermore, it could also be of considerable benefit for running multiple probabilistic scenarios and analyzing time-dependent behavior in an integrated MV to LV level model. Such a model could utilize the simplified LV approach in place of some of the fully detailed versions so as to reduce the overall computational complexity. In addition, it facilitates a better understanding of the influence that different variables have on overvoltage.

The accuracy of the model has been analyzed using data from a real distribution network comprising 10,213 LV areas. It has been shown that approximately 96% of the areas could be accurately modeled using the simplified model, with less than a 0.3% maximum absolute error in the estimated overvoltage values under balanced conditions with no load. When the effect of load was incorporated for a large subset of areas containing only residential loads, the error increased slightly, predominantly at low and medium penetration levels.

Finally, the model has been applied to investigate the benefits of reactive power injection across an entire distribution network. It has been shown that using only reactive power injection in this network has a limited effect on overall overvoltage levels and the number of non-compliant areas. Thus, it is difficult to justify using measures that only impose reactive power capabilities, without a broader consideration of other methods such as active power control/limitation which could also be investigated with the proposed model. Analogous results are expected for similar distribution networks.

References

[1] F. T. Manol Rekinger, "Global market outlook for solar power 2015-2019," SolarPower Europe, Brussels, Belgium, Tech. Rep. 9789082228410, 2015.

[2] M. H. J. Bollen and F. Hassan, *Integration of Distributed Generation in the Power System*, vol. 80. Hoboken, NJ, USA: Wiley, 2011.

[3] P. P. Barker and R. W. de Mello, "Determining the impact of distributed generation on power systems. I. Radial distribution systems," in *Proc. IEEE Power Eng. Soc. Summer Meeting*, vol. 3. Seattle, WA, USA, 2000, pp. 1645–1656.

[4] IEA-PVPS, "High penetration of PV in local distribution grids," Int. Energy Agency Task 14, Paris, France, Tech. Rep. IEA PVPS T14-02:2014, 2014. [Online]. Available: http://www.iea-pvps.org/

[5] M. Braun *et al.*, "Is the distribution grid ready to accept large-scale photovoltaic deployment? State of the art, progress, and future prospects," *Progr. Photovolt. Res. Appl.*, vol. 20, no. 6, pp. 681–697, 2012.

[6] N. Hatziargyriou, and C. Andrieu, "Benchmark systems for network integration of renewable and distributed energy resources," CIGRE Task Force C6.04, vol. 6, 2009.

[7] R. Tonkoski, D. Turcotte, and T. H. M. El-Fouly, "Impact of high PV penetration on voltage profiles in residential neighborhoods," *IEEE Trans. Sustain. Energy*, vol. 3, no. 3, pp. 518–527, Jul. 2012.

[8] K. Wang, F. Ciucu, C. Lin, and S. H. Low, "A stochastic power network calculus for integrating renewable energy sources into the power grid," *IEEE J. Sel. Areas Commun.*, vol. 30, no. 6, pp. 1037–1048, Jul. 2012.

[9] C.-L. Su, "Stochastic evaluation of voltages in distribution networks with distributed generation using detailed distribution operation models," *IEEE Trans. Power Syst.*, vol. 25, no. 2, pp. 786–795, May 2010.

[10] S. Conti and S. Raiti, "Probabilistic load flow using Monte Carlo techniques for distribution networks with photovoltaic generators," *Sol. Energy*, vol. 81, no. 12, pp. 1473–1481, 2007.

[11] W. H. Kersting, *Distribution System Modeling and Analysis*. Boca Raton, FL, USA: CRC Press, 2012.

[12] E. Muljadi, S. Pasupulati, A. Ellis, and D. Kosterov, "Method of equivalencing for a large wind power plant with multiple turbine representation," in *Proc. IEEE Power Energy Soc. Gen. Meeting—Convers. Del. Elect. Energy 21st Century*, Pittsburgh, PA, USA, 2008, pp. 1–9.

[13] WECC, Renewable Energy Modeling Task Force, "WECC guide for representation of photovoltaic systems in large-scale load flow simulations," *WECC Modeling and Validation Work Group*.

[14] M. J. Reno, R. J. Broderick, and S. Grijalva, "Formulating a simplified equivalent representation of distribution circuits for PV impact studies," Sandia Nat. Lab., Albuquerque, NM, USA, Tech. Rep. SAND2013-2831, 2013.

[15] M. J. Reno, K. Coogan, R. Broderick, and S. Grijalva, "Reduction of distribution feeders for simplified PV impact studies," in *Proc. IEEE 39th Photovolt. Spec. Conf. (PVSC)*, Tampa, FL, USA, Jun. 2013, pp. 2337–2342.

[16] G. Kerber and R. Witzmann, "Statistical distribution grid analysis and reference network generation," *EW Mag.*, vol. 107, no. 6, pp. 22–26, 2008.

[17] B. Bletterie *et al.*, "Characterising LV networks on the basis of smart meter data and accurate network models," in *Proc. Integr. Renew. Distrib. Grid CIRED Workshop*, Lisbon, Portugal, 2012, pp. 1–4.

[18] A. Kimber *et al.*, "Improved test method to verify the power rating of a photovoltaic (PV) project," in *Proc. 34th IEEE Photovolt. Spec. Conf. (PVSC)*, Philadelphia, PA, USA, Jun. 2009, pp. 000316–000321.

[19] L. M. Hajagos and B. Danai, "Laboratory measurements and models of modern loads and their effect on voltage stability studies," *IEEE Trans. Power Syst.*, vol. 13, no. 2, pp. 584–592, May 1998.

[20] A. J. Collin, "Advanced load modelling for power system studies," Ph.D. dissertation, School Eng., Univ. Edinburgh, Edinburgh, U.K., 2013.

[21] *IEC Standard Voltages*, IEC Standard 60038, 2009.

[22] VDE Association for Electrical, Electronic and Information Technologies. (Nov. 2012). *VDE-AR-N 4105:2011-08 Power Generation Systems Connected to the Low-Voltage Distribution Network*. [Online]. Available: https://www.vde.com/de/InfoCenter/Seiten/Details.aspx?eslShopItemID=0d65ed5e-83c9-4d84-af92-356f06b66f8b

[23] T. Stetz, *Autonomous Voltage Control Strategies in Distribution Grids With Photovoltaic Systems: Technical and Economic Assessment*, vol. 1. Kassel, Germany: Kassel Univ. Press GmbH, 2014.

[24] P. Esslinger and R. Witzmann, "Evaluation of reactive power control concepts for PV inverters in low-voltage grids," in *Proc. Integr. Renew. Distrib. Grid CIRED Workshop*, Lisbon, Portugal, 2012, pp. 1–4.

David Santos-Martin received the B.Sc. degree in electrical and electronic engineering from ETSII-UPM, Madrid, Spain; the M.S. degree in control engineering from the École Supérieure d'Électricité, Paris, France; and the Ph.D. degree in electrical engineering from UC3M, Madrid. He was with Iberdrola and Ecotecnia-Alsthom. He is an Assistant Lecturer with the Department of Electrical Engineering, and a Researcher with the EPECentre, University of Canterbury, New Zealand.

Scott Lemon (S'13) received the B.E. degree (Hons.) in electrical and electronic engineering from the University of Canterbury, New Zealand, in 2013, where he is currently pursuing the Ph.D. degree. His research interests include renewable energy and the smart grid, computer-based simulation and visualization of complex systems, and embedded hardware development.